

Supplementary information for:

Visible-light photoelectric response in semiconducting quaternary oxysulfide FeOCuS with anti-PbO-type structure

Wei Du,^a Ganghua Zhang,^{*a,b} Ping Chen,^c Pingying Tang,^d Jing Wang,^a Dezeng Li,^c Jingshan Hou^{*a} and Yongzheng Fang^{*a}

^aSchool of Materials Science and Engineering, Shanghai Institute of Technology, Shanghai, 201418, P. R. China;

^bShanghai Key Laboratory of Engineering Materials Application and Evaluation, Shanghai Research Institute of Materials, Shanghai, 200437, P. R. China;

^cSchool of Electric, Shanghai Dianji University, Shanghai, 201306, P. R. China;

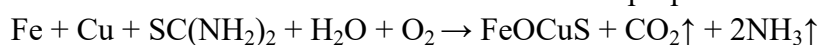
^dKey Laboratory of New Electric Functional Materials of Guangxi Colleges and Universities, Nanning Normal University, Nanning, 530023, P. R. China;

^eSchool of Chemistry and Molecular Engineering, East China Normal University, Shanghai, 200241, P. R. China.

Emails: ganghuazhang@sit.edu.cn (G.H. Zhang) hujingshan@hotmail.com (J.S. Hou) and fyz1003@sina.com (Y.Z. Fang)

Experimental

All chemicals were used without further purification. Single-crystal FeOCuS was synthesized via a hydrothermal method. Briefly, 10 mmol of Fe powder, 10 mmol of Cu powder, 1.9 g of $\text{SC}(\text{NH}_2)_2$, 15 g of LiOH and 20 mL distilled water were sequentially added in a beaker under continuous stirring and the solution was cooled to room temperature. The mixture was then transferred into a 50 mL Teflon-lined stainless-steel autoclave to fill 70% of its capacity. Crystallization was carried out under autogenous pressure at 200 °C for 2-3 days. After the autoclave was cooled and depressurized, the products were washed with absolute alcohol and sonicated using an SB2200 ultrasonic washing machine. And then, single-phase FeOCuS was obtained as a fine dark crystalline powder at the bottom of the beaker. In hydrothermal process, the possible chemical reactions play important roles in the formation of the final products. Herein, a redox reaction for the fabrication of FeOCuS was proposed as:



The crystal structure of FeOCuS was solved by single-crystal X-ray diffraction using an Enraf-Nonius Kappa CCD diffractometer with graphite-monochromatized $\text{Mo } K_\alpha$ ($\lambda = 0.71073 \text{ \AA}$) radiation following the ω - 2θ scan method. The absorption correction was applied using the SADABS program.¹ The structure was solved by the direct method and refined on F^2 by the full-matrix least-square method using the SHELXS-97 and SHELXL-97 programs, respectively.^{2,3} The purity and crystallinity of the sample were checked by powder X-ray diffraction collected on a Rigaku D/Max-2000 diffractometer with $\text{Cu } K_\alpha$ radiation ($\lambda = 1.5418 \text{ \AA}$) at 40 kV, 100 mA. The microstructure of FeOCuS was confirmed by transmission electron microscopy (TEM, carried out on a JEM2100F with an accelerating voltage of 200 kV). Scanning electron microscopy (SEM) and Energy Dispersive Spectroscopy (EDS) were performed on an FEI Quanta 200F microscope operating at 3 kV. The oxidation states of Fe, Cu, O and S atoms were confirmed by X-ray photoelectron spectroscopy (XPS) using an Axis Ultra spectrometer. The spectra were collected for C 1s, Fe 2p, Cu 2p, O 1s and S 2p regions, and the binding energies were corrected versus the C 1s reference of 284.5 eV.

The optical property of the sample was analyzed using a UV-3100 Shimadzu ultraviolet-visible-infrared spectrophotometer equipped with an integrating sphere in reflectance mode. Thermogravimetric analysis (TGA) was carried out on a Q50 (TA Instruments) thermal analyzer with a heating rate of 10 K min^{-1} from room temperature to 1073 K under a nitrogen atmosphere. The low temperature magnetic property of FeOCuS was studied by using a quantum design physical property measurement system (PPMS). The DC susceptibility measurements, both under zero-field-cooling (ZFC) and field-cooling (FC) conditions, were performed in a 100 Oe magnetic field for temperatures ranging from 5 to 300 K. For temperature-dependent resistance and photoelectric measurements, the ceramic sample was prepared by grinding powders (crystallites) and pressing them into pellets with a diameter of 7 mm under a pressure of 10 MPa. Pellets were next sealed in vacuumized quartz tubes and sintered into ceramics by sintering at 553 K for 10 h. The temperature variation of the resistivity, $\rho(T)$, was measured using the standard four-probe technique collected on PPMS. The

photoelectric performance of the ceramic sample was measured by an interactive source meter instrument (Model 2450, Keithley), under solar-light irradiations with a 500 W Xenon lamp.

All theoretical calculations have been implemented in the Vienna *ab initio* simulation package (VASP).^{4,5} The Heyd-Scuseria-Ernzerhof hybrid functional (HSE06)^{6,7} is used in the density of states (DOS) and band calculations. The energy cutoff for plane wave is set to 550 eV. A $6 \times 6 \times 4$ Monkhorst-Pack is used for the Brillouin-zone integration.⁸ The relaxation of electronic degrees of freedom is stopped if the total energy changes within 10^{-5} eV/atom. For the band calculation, the selected K-points path is Z (0.0, 0.0, 0.5) \rightarrow A (0.5, 0.5, 0.5) \rightarrow M (0.5, 0.5, 0.0) \rightarrow G (0.0, 0.0, 0.0) \rightarrow Z (0.0, 0.0, 0.5) \rightarrow R (0.0, 0.5, 0.5) \rightarrow X (0.0, 0.5, 0.0) \rightarrow G (0.0, 0.0, 0.0).

References:

1. Sheldrick and G.M. SADABS. Version 2007/2, (Bruker AXS Inc., Madison, Wisconsin, USA, 2007).
2. Sheldrick and G.M, SHELXS97, Program for Solution of Crystal Structures. (University of Göttingen, Göttingen, Germany, 1997).
3. Sheldrick and G.M, SHELXL97, Program for Solution of Crystal Structures. (University of Göttingen, Göttingen, Germany, 1997).
4. G. Kresse and J. Furthmüller, *Comp. Mater. Sci.*, 1996, **6**, 15-50.
5. G. Kresse and J. Furthmüller, *Phys. Rev. B*, 1996, **54**, 11169-11186.
6. J. Heyd, J. E. Peralta and G. E. Scuseria, *J. Chem. Phys.*, 2005, **123**, 174101.
7. A. V. Krukau, O. A. Vydrov, A. F. Lzmaylov and G. E. Scuseria, *J. Chem. Phys.*, 2006, **125**, 224106.
8. H. J. Monkhorst and J. D. Pack, *Phys. Rev. B*, 1976, **13**, 5188-5192.

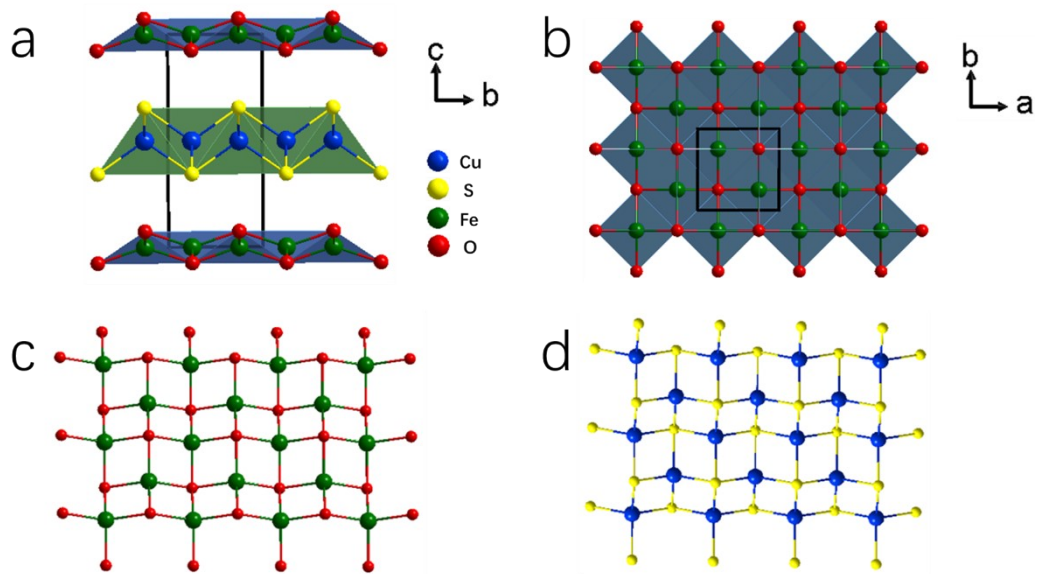


Fig. S1 Schematic polyhedral structure model of FeOCuS with space group $P_{4/nmm}$ viewed along a (a) and c -axis (b), respectively. The separate view for FeO_4 (c) and CuS_4 (d) layers of FeOCuS viewed along c -axis.

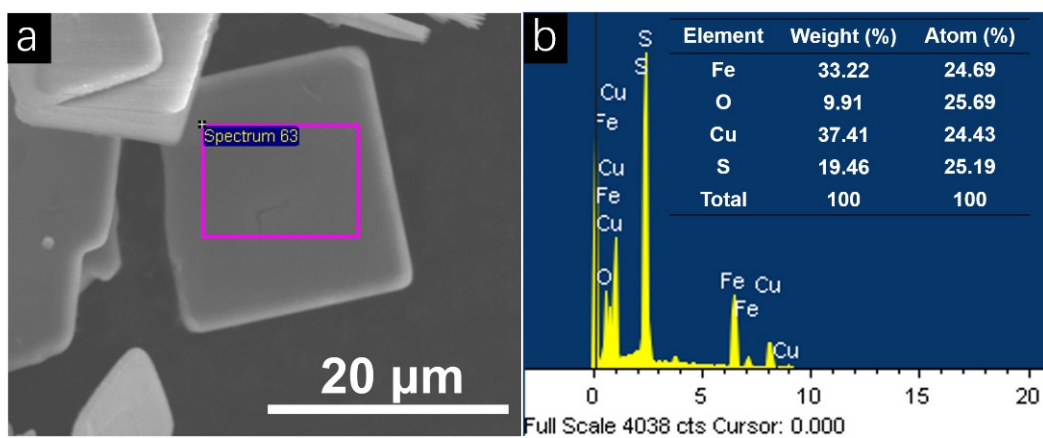


Fig. S2 (a) SEM image of crystalline sample for FeOCuS and (b) EDX result of FeOCuS.

Basic Experiment Information								
Order Number	2110272508							
Test Items	Fe, Cu, S							
Number of Samples	1							
Test Date	2021/10/30							
Instrument Model	Agilent 720ES							
Instrument Parameters	RF Power: 1.20KW							
	Plasma flow: 15.0L/min							
	Auxiliary flow: 1.50L/min							
	Nebulizer flow: 0.75L/min							
	Sample uptake delay: 15s							
	Instr stabilization delay: 15s							
	Replicate read time: 2s							
Replicates: 3 times								
Data								
Sample	Sample mass m_0 (g)	Constant volume V_0 (mL)	Test items	Initial concentration C_0 (mg/L)	Dilution ratio f	Element content in Test Solution C_1 (mg/L)	Element content in sample C_x (mg/kg)	Wt%
1	0.0504	10	Cu	13.48	100	1347.70	267400.79	26.74%
	0.0504	10	Fe	12.12	100	1211.63	240402.78	24.04%
	0.0504	10	S	6.64	100	663.76	131698.66	13.17%

Fig. S3 The ICP-OES results for the sample.

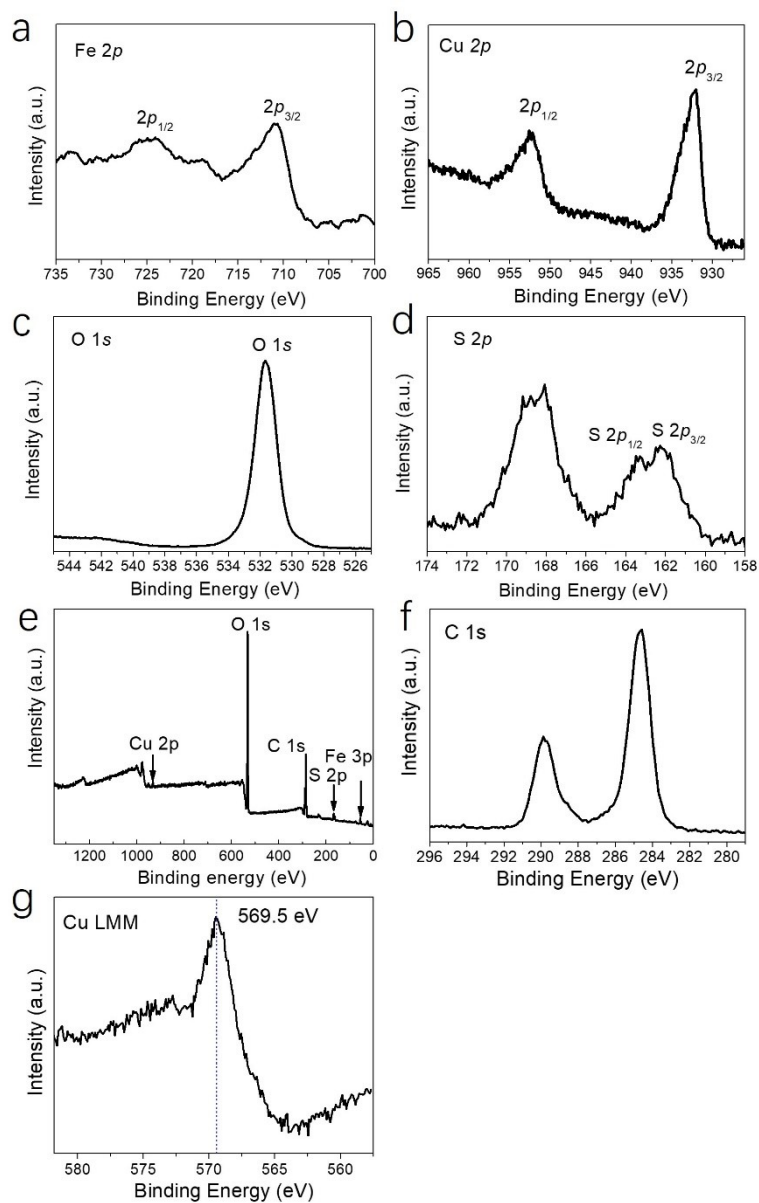


Fig. S4 XPS spectra of FeOCuS: (a) for Fe $2p$, (b) for Cu $2p$, (c) for O $1s$, (d) for S $2p$, (e) for survey XPS spectra and (f) for C $1s$ reference. (g) The Auger Cu LMM spectrum for FeOCuS.

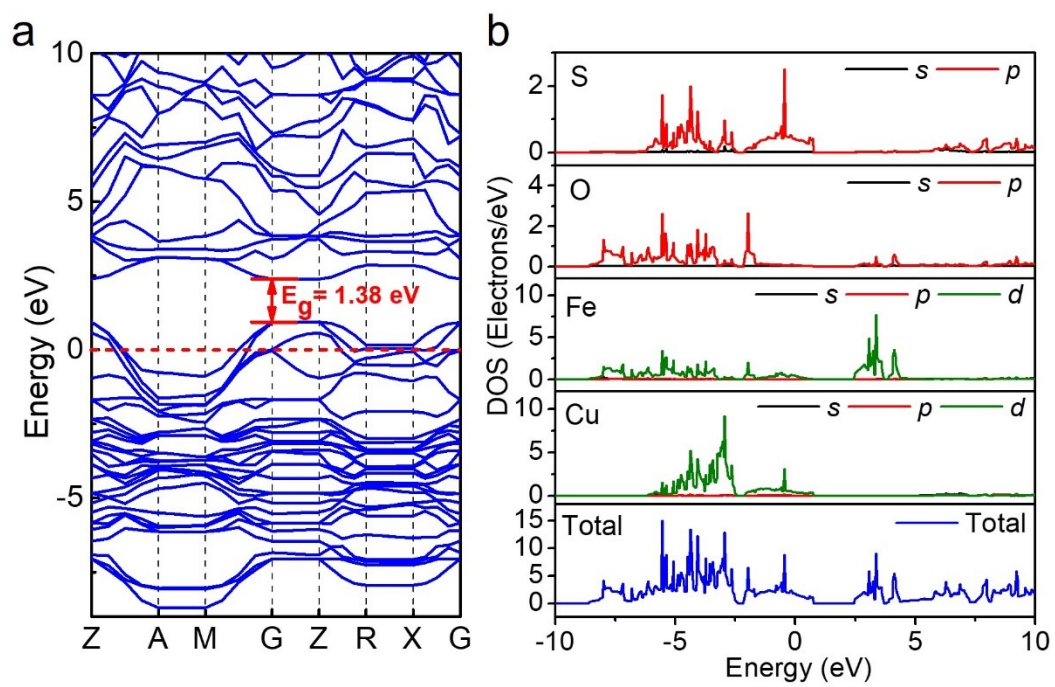


Fig. S5 Band structure (a) and DOS (b) of FeOCuS.

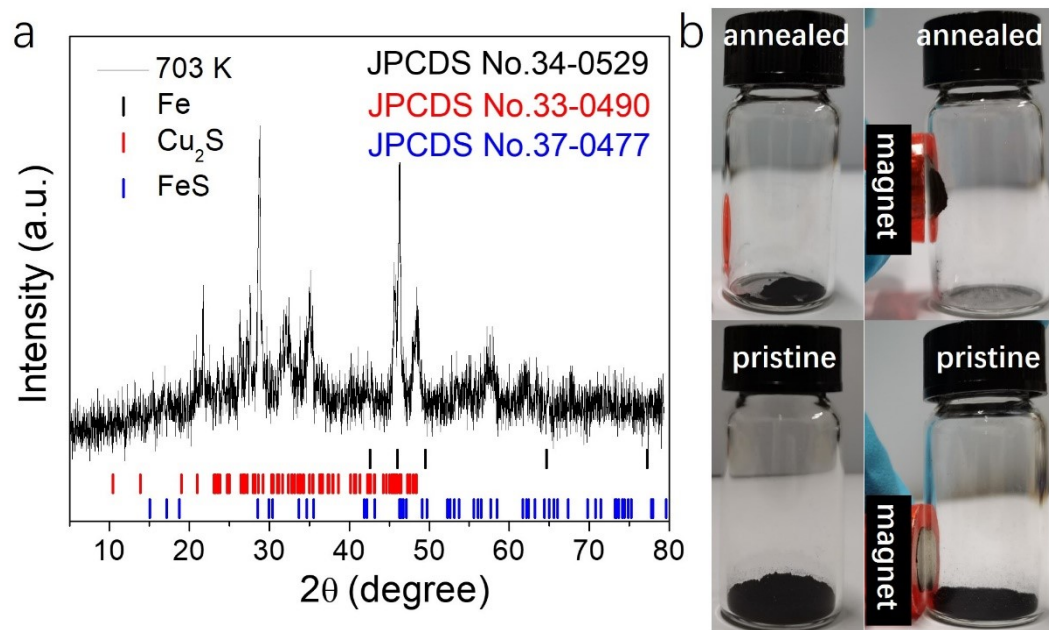


Fig. S6 (a) The powder XRD of FeOCuS samples annealed at room temperature (RT) and 703 K. (b) The optical photographs for the annealed and pristine samples responding to an external magnetic field.

It can be found that ZFC and FC curves give a distinct separation at low temperature, suggesting the existence of a weak ferromagnetic contribution. For both ZFC and FC curves, the magnetic moment initially increases monotonously with decreasing the temperature, and then suddenly drops at 19 K for FC and 34 K for ZFC, respectively. Considering the magnetic field dependent behaviour, these broad peaks should be assigned to the superparamagnetic blocking temperature (T_B) or the spin-glass freezing temperature (T_f) rather than the Néel temperature (T_N). For a high spin Fe^{3+} ion ($3d^5$, high-spin state, $S = 5/2$, $g_J = 2$), the theoretical spin-only value can be calculated from $\mu_{eff} = g_J [S(S + 1)]^{1/2} \mu_B = 5.92 \mu_B$. For Cu^+ ions, μ_{eff} are equal to 0 due to its nonmagnetic nature. Thus, the effective paramagnetic moment of FeOCuS can be calculated with the formula: $\mu_{cata} = (\mu(\text{Fe}^{3+})^2 + \mu(\text{Cu}^+)^2)^{1/2} = 5.92 \mu_B$, which is in good agreement with the experimental one determined from $1/\chi$ vs. T plot at high temperatures.

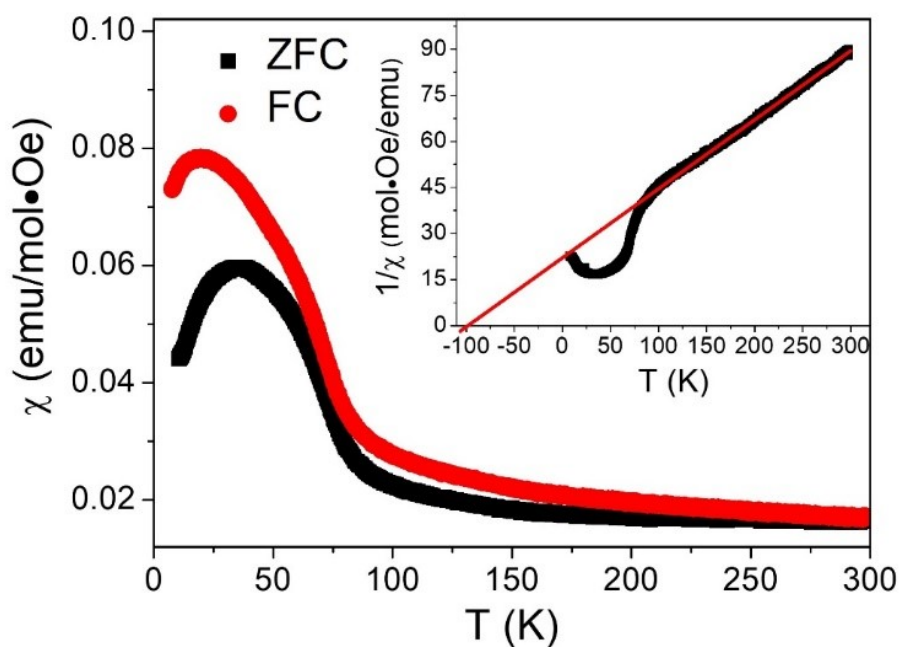


Fig. S7 χ versus T curves for FeOCuS were obtained by PPMS under both ZFC and FC models recorded in temperature range from 5 to 300 K at 100 Oe applied field (the inset shows the $1/\chi$ vs. T plot).

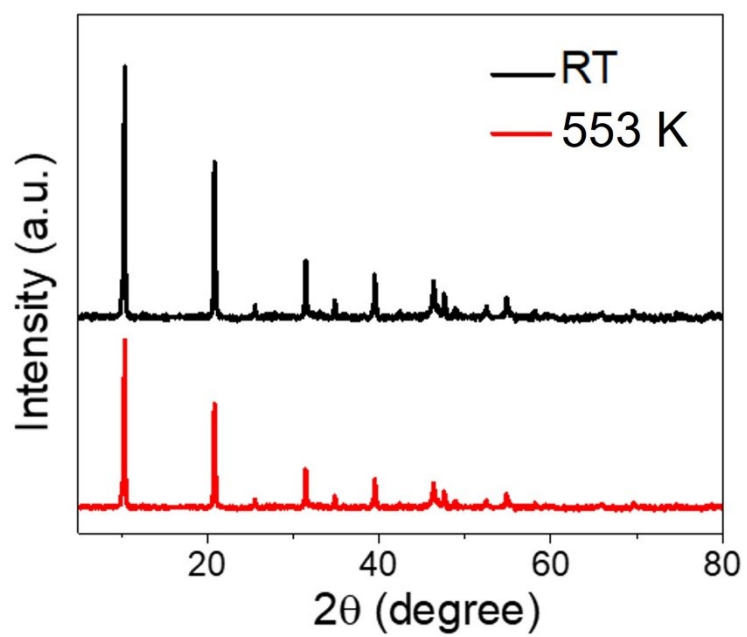


Fig. S8 The powder XRD of FeOCuS samples annealed at room temperature (RT) and 553 K.

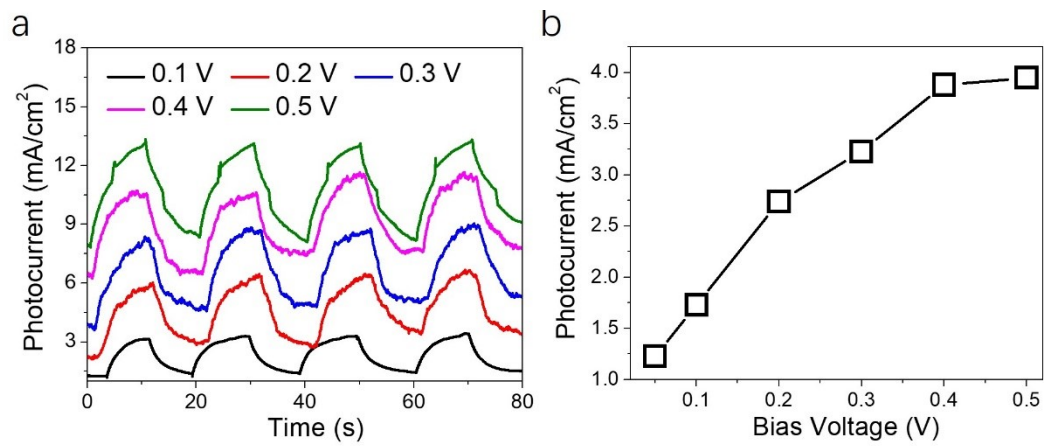


Fig. S9 (a) The photocurrent-time (I - T) curves of FeOCuS at different bias voltages following on-off visible-light exposure. (b) The corresponding bias-dependent photocurrent.

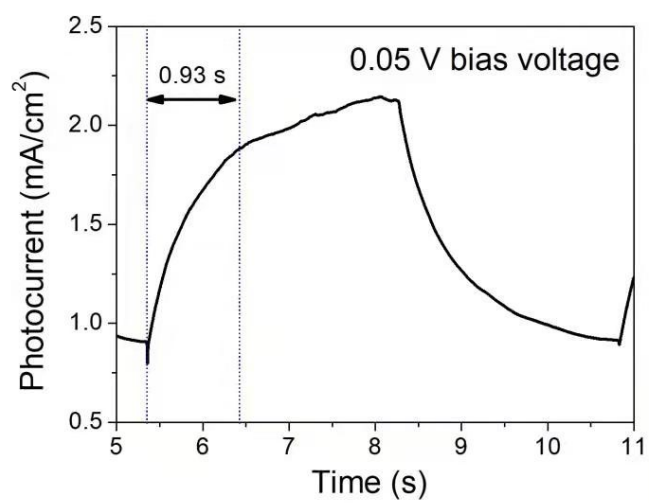


Fig. S10 The corresponding response time of FeOCuS at 0.05 V bias voltage.

Table S1 Crystal data and structure refinement parameters for FeOCuS single crystal.

Empirical formula	FeOCuS
F_w (g·mol ⁻¹)	167.46
T (K)	296
λ (Å)	0.71073
Crystal system	tetragonal
Space group	P _{4/nmm}
a (Å)	3.8219(5)
b (Å)	3.8219(5)
c (Å)	8.645(3)
$\alpha=\beta=\gamma$ (deg)	90
V(Å ³)	126.28(5)
Z	2
D _{calc} (g/cm ³)	4.404
μ (mm ⁻¹)	14.625
Goodness-of-fit on F^2	1.066
R1, wR2 [$I > 2\theta(I)$]	0.0542, 0.1296
R1, wR2 [all data]	0.0587, 0.1336

Table S2 Structural parameters of FeOCuS single crystal at room temperature.

Atom	x	y	z	g	$U_{\text{iso}}(\times 100\text{\AA}^2)$
Cu	0.75	0.25	0.5	1	19.9
S	0.25	0.25	0.3442	1	12.3
Fe	0.25	0.75	1.0	1	19.0
O	0.25	0.25	0.9256	1	20.0
Selected bond length (Å)					
Fe—O	2.0163(36)				
Cu—S	2.3379(20)				
Selected bond angle (°)					
$\angle\text{O-Fe-O}$	95.840(3)	$\angle\text{O-Fe-O}$	142.796(3)		
$\angle\text{S-Cu-S}$	109.384(3)	$\angle\text{S-Cu-S}$	109.646(2)		

U_{iso} is the isotropic thermal parameter, g is the occupation factor.

Generally, three models have been adopted to describe the semiconducting transport. One is classical thermal activation (TA) model in which $\rho(T)$ is expressed as $\rho = \rho_0 \cdot \exp(E_A/k_B T)$, where ρ_0 is the value of resistivity at infinite temperature, E_A is the activation energy and k_B is the Boltzmann constant. The second one is the small polaron hopping (SPH) model in which $\rho(T)$ is expressed as $\rho(T) = AT \exp(E_A/k_B T)$, where A is a constant.¹ The third one is the variable range hopping (VRH) model where $\rho(T)$ is expressed as $\rho(T) = \rho_0 \exp(T_0/T)^{1/4}$; where ρ_0 is the residual resistivity and T_0 is the characteristic temperature.²

In the VRH case, charge transport can be considered as a combination of tunneling process and thermal activation supplied by the phonons. The site that the electrons will hop to is above the Fermi level from the original site, which has minimum energy difference irrespective of the spatial distance. Therefore, the density of states is considered as a constant around the Fermi energy in Mott's VRH process. The hopping length (R) and the hopping energy (W) should vary with the temperature, which should follow the below given formulae:²

$$R = \left(\frac{9}{8\pi\alpha N(E_f)k_B T} \right)^{\frac{1}{4}} \quad (1)$$

$$W = \left(\frac{3}{4\pi R^3 N(E_f)} \right) \quad (2)$$

$$T_0 = \frac{\lambda\alpha^3}{k_B N(E_f)} \quad (3)$$

$$\frac{1}{\rho_0} = 3e^2 v_{ph} \left(\frac{N(E_f)}{8\pi\alpha k_B} \right)^{\frac{1}{2}} \quad (4)$$

Where, α is the inverse fall-off length of the wavefunction, λ is a dimensionless constant (~ 18.1), e is the electronic charge, v_{ph} is an optical phonon frequency ($\sim 10^{13}$ Hz), $N(E_f)$ is the density of states at the Fermi level, k_B is the Boltzmann constant. With the values of T_0 and ρ_0 , the values of α and $N(E_f)$ (given in **Table S3**) can be calculated from the equations (3) and (4). Consequently, the values of R and W at different temperature can be evaluated from the above formulae (1) and (2).

Table S3 Fitting parameters obtained from resistivity data for FeOCuS.

Compound	TA model		VRH model			
	E_A (eV)	ρ_0 ($\Omega \cdot \text{cm}$)	T_0 (K)	ρ_0 ($\Omega \cdot \text{cm}$)	α^{-1} (nm)	$N(E_f)$ ($\text{eV}^{-1} \text{cm}^{-3}$)
FeOCuS	0.004	6.1148	7.8×10^2	1.9705	5.35×10^{-22}	1.77×10^{66}

References:

1. N. F. Mott and E. A. Davis, *Electrical Process in non-crystalline materials*, Clarendon Press, Oxford, 1971.
2. N. F. Mott, *J. Non-Cryst. Solids*, 1972, **8**, 1-18.